Available online at www.sciencedirect.com
ScienceDirect
Ceramics International 34 (2008) 69–74
CERAMICS INTERNATIONAL
www.elsevier.com/locate/ceramint

# Synthesis and cathodoluminescence properties of porous wood (fir)-templated zinc oxide

Zhaoting Liu [a], Tongxiang Fan [a], Jian Ding [a], Di Zhang [a,*], Qixin Guo [b], Hiroshi Ogawa [b]

[a] State Key Lab of Metal matrix Composites, Shanghai Jiaotong University, 200030 Shanghai, PR China
[b] Department of Electrical and Electronic Engineering, Saga University, Saga 840-8502, Japan

Received 17 May 2006; received in revised form 9 July 2006; accepted 18 August 2006
Available online 17 October 2006

**Abstract**

Wood (fir)-templated ZnO with hierarchically porous structure has been successfully synthesized through a simple hydrothermal process. Morphology and porosity of the products were investigated by FESEM, TEM, and $N_2$ adsorption, respectively. The optical properties were measured by cathodoluminescence (CL) at room temperature. The morphologies of bulk and ground flake ZnO show an inheritance from the fir microstructure. Experimental results suggest that a higher calcination temperature will influence the grain size and porosity. The pore size decreases from 20 to 10 μm in the bulk ZnO, while increases from 50 nm to several micrometers in the flake ZnO when the calcination temperature changes from 600 to 1200 °C. CL spectra also show temperature-dependent properties at ultraviolet (UV) band and blue band. The intensity of visible emission originated from oxygen vacancies is proportional to the calcination temperature, while that of UV emission is inverse proportional due to quantum confinement effect.


*Keywords:* B. Porosity; C. Optical properties; D. ZnO; Wood template

## 1. Introduction

Zinc oxide (ZnO) is well known for its electrical, optoelectronic and photochemical properties and high chemical stability; it has a wide band gap (3.37 eV) and a high exciton binding energy of 60 meV. It is a promising candidate for optical, piezoelectric, ferroelectric, ferromagnetic applications. Because of its applicability to laser diodes and light emitting diodes in the UV-blue region [1,2], there have been many studies on the luminescence of ZnO under various excitation sources such as photoluminescence (PL) and cathodoluminescence (CL). Compared with PL, CL has the advantage of a much higher lateral and depth resolution due to the smaller possible diameter of the exciting electron beam of only some 10 nm and the adjustable electron energy in the keV range, respectively [3]. Recently, different synthesis methods have been employed to produce ZnO ceramics with various morphologies. Pan et al. [4] prepared ultralong ZnO nanobelt with a rectanglelike cross section by thermal evaporating the commercial zinc oxide. ZnO nanowire arrays have been fabricated by Zhang et al. [5] by electrochemical deposition technique based on ordered nanoporous alumina membrane. Similar ZnO nanowires were prepared by Fan et al. [6] through template-directed method for large-scale fabrication of hexagonally patterned and vertically aligned. By metalorganic chemical vapor deposition, Zhang et al. [7] fabricated ZnO rods directly on sapphire (0 0 0 1) substrates which exhibited free exciton and bound exciton emissions at low temperatures. However, most of these methods need special equipment or complex process control, and few techniques for producing ZnO preforms with reticulate and hierarchically porous structures have been reported till now.

Here we report a new simple synthesis method for fir-templated ZnO with a retained structure from natural fir wood template, together with the product's CL property. Bio-templated process, one area of biomimetic technology [8], is a process of *in situ* modification with natural biological materials, to keep unique and natural structures of bio-templates, which are different from traditional man-made products. Wood is suitable as a kind of template owing to its

* Corresponding author.
*E-mail address:* Zhangdi@sjtu.edu.cn (D. Zhang).

0272-8842/$32.00 
doi:10.1016/j.ceramint.2006.08.006

highly and hierarchically porous structure. It has a mm scale of growth ring and vessel pore, a μm scale of transverse ray parenchyma, longitudinal tracheid and fiber, and even a nm scale of molecular fiber and cell membrane [9]. Some groups have fabricated wood-templated porous ceramics, such as carbide ceramics (SiC [10–13], TiC [14], etc.), oxide ceramics ($Fe_2O_3$ [15], NiO [16], $Al_2O_3$ [17], and $TiO_2$ [17,18]), and composites (SiOC/C [19], and SiSiC [20]), etc. We used fir softwood, as shown in Fig. 2(a), a kind of coniferous wood, as template to synthesize ZnO because of its uniformly porous microstructure. Fir is composed of a unique cross-sectional constructed cell called tracheid cell, which accounts for over 90% in wood volume, and bordered pits along the tracheid walls for tangential connectivity. Most of former researches in this area are still concentrated on the synthesis and the mechanical properties of bio-templated materials, and their photoelectrical property has been scarcely reported. In the present study, the morphology and CL properties of fir-templated ZnO calcined at different temperatures of 600, 800, 1000 and 1200 °C are investigated.

## 2. Experimental

The pieces of fir wood with size 2 cm × 1 cm × 0.3 cm were heated in boiling 5% dilute ammonia for 6 h to get rid of the gums, fats and fatty acids in the wood. Extracted wood templates, which contain better connectivity and cellular affinity for the penetration of precursor solution, were washed by deionized water and dried at 80 °C for 24 h. The precursor solution was prepared from zinc nitrate, ethanol and deionized water with the ratio of 4 mmol:2 ml:1 ml. The solvent, ethanol also as surfactant provided enough $OH^-$ for nitrate hydrolysis. Then the dry wood specimens were infiltrated in the precursor sol at 60 °C in covered beakers. When the samples were infiltrated for 24, 48 and 72 h, respectively, their infiltration rates were 47%, 74% and 107%. So 72 h were chosen as the infiltration time here for getting high infiltration rate to preserve the wood's structure well. After the specimens were taken from the solution, they were air-dried for another 24 h at 60 °C. Finally, the specimens were then calcined at the temperatures of 600, 800, 1000 and 1200 °C for 2 h in air atmosphere and air-cooled to room temperature.

Some bulk ZnO samples obtained were ground with an agate mortar. Field emission scanning electron microscope (FESEM) was performed by FEI SIRION200 and PHILIPS XL30 FEG scanning electron microscope to investigate the morphology of both bulk and ground samples. The crystal structures were characterized by X-ray diffraction (XRD, Cu Kα radiation in JEOL JDX-3530). Transmission Electron Microscope (TEM) observation was performed with a FEI Technai G2 microscope. Pore size distributions (PSD) were measured by a Micromertitics ASAP 2010 nitrogen adsorption analyzer at liquid nitrogen temperature. Cathodoluminescence (CL) measurements were conducted in FEI XL30 equipped with a MonoCL2 system designed by Oxford Research Instruments at room temperature. A photomultiplier (Hamamatsu, R316-02) was used to detect luminescence with electron beam voltage of 15 kV.

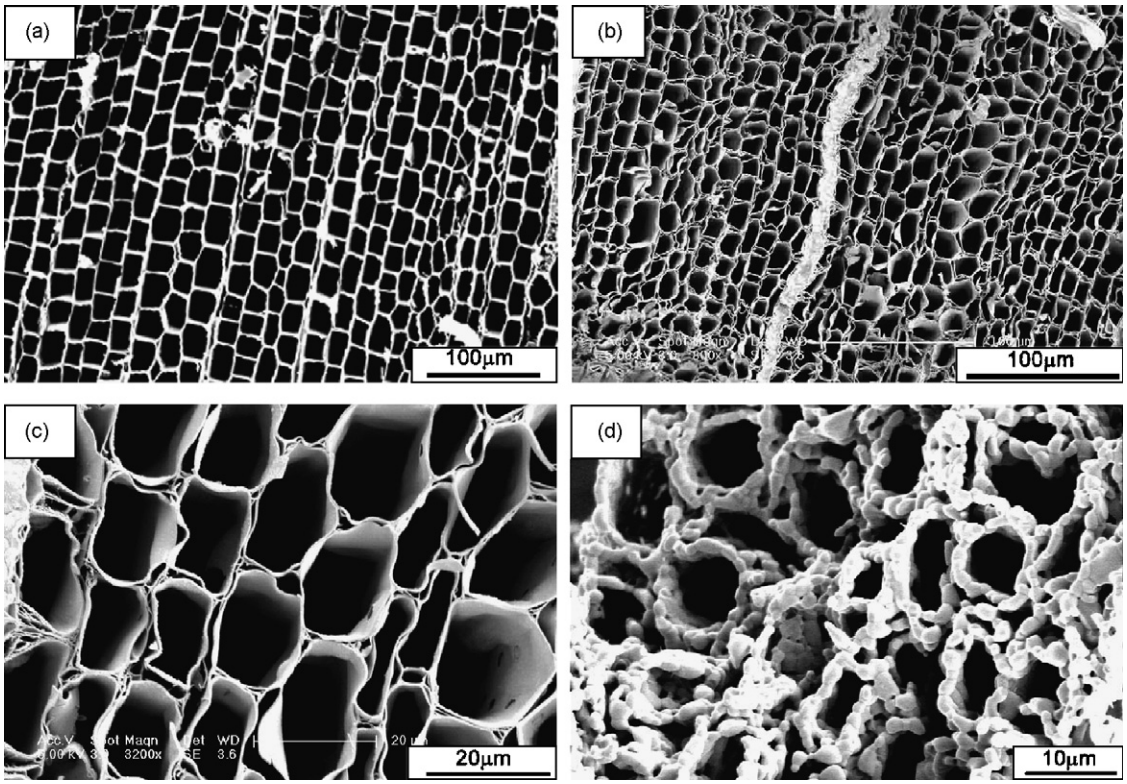


Fig. 1. FESEM images of the cross sections of (a) fir char template pyrolyzed at 600 °C in vacuum condition; (b and c) fir-templated ZnO sample (before grinding) calcined at 600 °C; (d) calcined at 1200 °C.

## 3. Results and discussion

Fig. 1(a) shows the morphology of fir char template pyrolyzed at 600 °C for 2 h in vacuum condition in FESEM images. The rectangle tracheid cells consist of the cross section of fir wood with a diameter of about 20 μm. The cross sections of fir-templated ZnO calcined at 600 °C are shown in Fig. 1(b) and (c) separately with different magnifications. In comparison with char template, fir-templated ZnO has reproduced the array of tracheid cells from fir wood with similar cell diameters to char template and shown the cell's topologically uniform arrangement. During infiltration, the cell walls of the wood adsorbed zinc precursor solution through capillary adsorption by wood's channels and fibers. From the view of the cell array (see Fig. 1(b)), due to the zinc precursor deposited on every cell wall homogeneously, the porous structural feature of fir wood was maintained by obtained ZnO after initial components of wood were burn out. From the view of a single cell (see Fig. 1(c)), the zinc precursor could not disperse uniformly through the single cell wall because of the thickness of wall and most of them deposited on the cell surface, which caused some cracks between cells in final ZnO sample as shown in Fig. 1(c). While the calcination temperature of fir-templated ZnO raised up to 1200 °C, as shown in Fig. 1(d), the initial cellular anatomy could not be reproduced faithfully and the pore diameters decreases obviously to about 10 μm because of the thermal contraction severely and grain growth to the size in μm-scale. However, the porous structure can be obtained owing to the contribution of wood template.

Fig. 2 shows the XRD patterns of the fir-templated ZnO obtained at calcination temperatures of 600, 800, 1000 and 1200 °C, respectively. Hexagonal ZnO was the only detectable phase in the powder samples. No diffraction patterns of initial wood components such as carbon were found, which means carbon has been removed completely during the process of heat treatment.

Bulk ZnO calcined at 1000 °C was ground into flakes in the agate mortar as shown in the high resolution FESEM images (see Fig. 3). Hollow tubular structure, the characteristics of tracheid, is distinguished in the flakes of the product as shown in inserted image. The cell wall of tracheid shown in Fig. 3 is composed of uniform and round ZnO particles with the size of several hundred nm. A hole of about 2 μm surrounded by ZnO particles is retained from Fir's pit structure. According to the FESEM image, the conclusion can be induced that partial microstructural features of fir template such as tracheid and pit were preserved even after ZnO products were ground and this kind of microstructure can make fir-templated ZnO hierarchical porous and well connective.

Further evidence about the crystallization of flake ZnO products is provided by TEM images in Fig. 4(a) and (b). The sample calcined at 600 °C (see Fig. 4(a)) shows that the fine spherical ZnO particles have the size of about 20–50 nm. There are many pores dispersed uniformly with the similar diameter to the particles each of which was surrounded by several ZnO particles. Fig. 4(b) shows the HRTEM image of an edge of the spherical particle as marked by a box in Fig. 4(a), and Fast Fourier transformation (FFT) of the digitalized HRTEM image is inserted. FFT analysis indicates the HRTEM was taken close to the [0 0 1] zone axis. The distance between the adjacent lattice fringes is measured about 0.28 nm on HRTEM image, which reveals the fringes of (100) planes according to the ZnO crystal ($a = 0.325$ nm, $c = 0.521$ nm).

Fig. 5(a) and (b) shows the $N_2$ adsorption isotherms and PSD plots of flake ZnO calcined at different temperatures. The isotherm of 600 °C sample corresponds to type IV curve caused by the capillary condensation of mesopores based on the IUPAC classification of isotherms, and according to the PSD plot its mesopores have the major diameter of about 50 nm in agreement with the TEM observation. A type H3 hysteresis loop (see IUPAC classification of hysteresis loops) indicates the asymmetric slot shape of mesopores or channels in coincidence with the tubular characteristics of the wood's pores. On the other side, a narrow hysteresis loop illustrates an interconnected mesoporous system and very high pore connectivity according to the percolation theory [21]. The shape of the isotherm without the knee of desorption plot is attributed to the existence of some macropores full of nitrogen vapour that nitrogen can

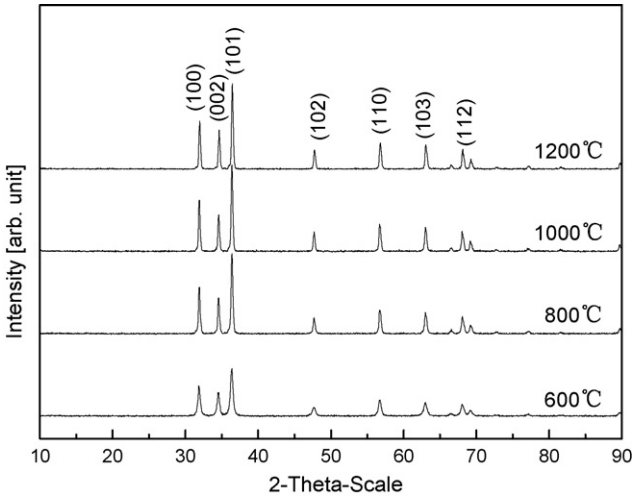


Fig. 2. XRD patterns of the fir-templated ZnO samples calcined at 600 °C, 800 °C, 1000 °C and 1200 °C, respectively.

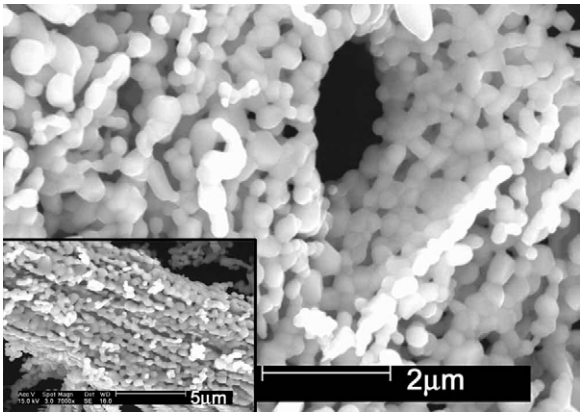


Fig. 3. FESEM image of the fir-templated ZnO sample (after grinding) calcined at 1000 °C.

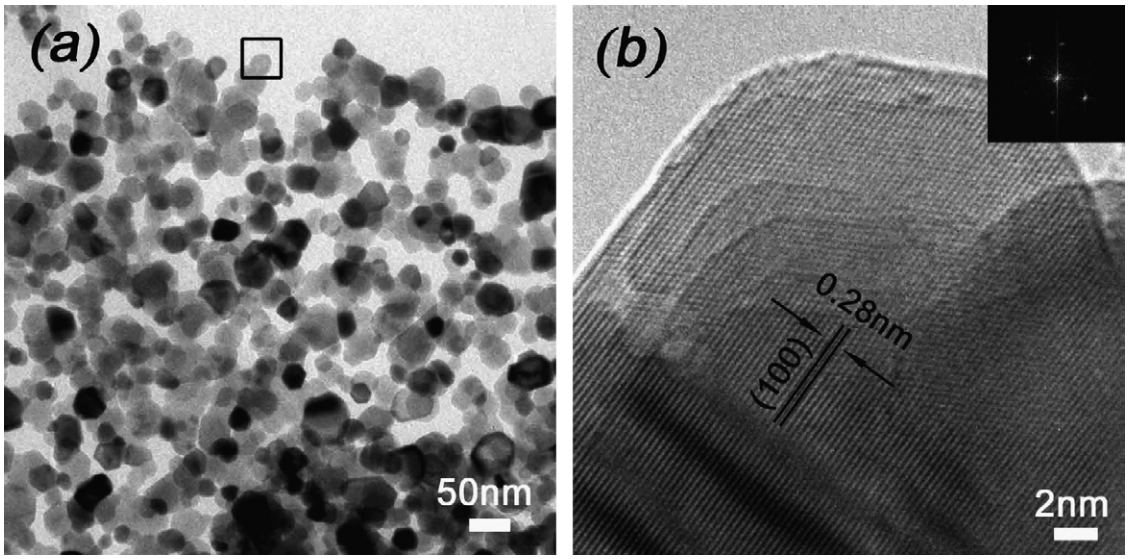


Fig. 4. (a) TEM images of the fir-templated ZnO sample calcined at 600 °C. (b) A typical HRTEM image of the sphere wall as marked by a box in (a). Inset: FFT image of the HRTEM image.

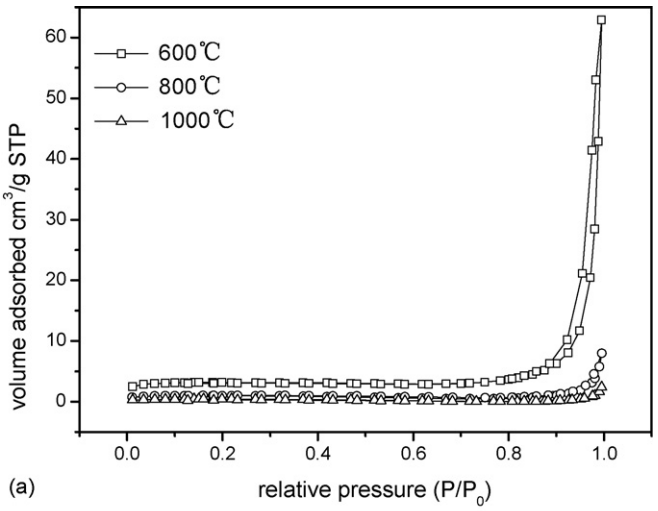


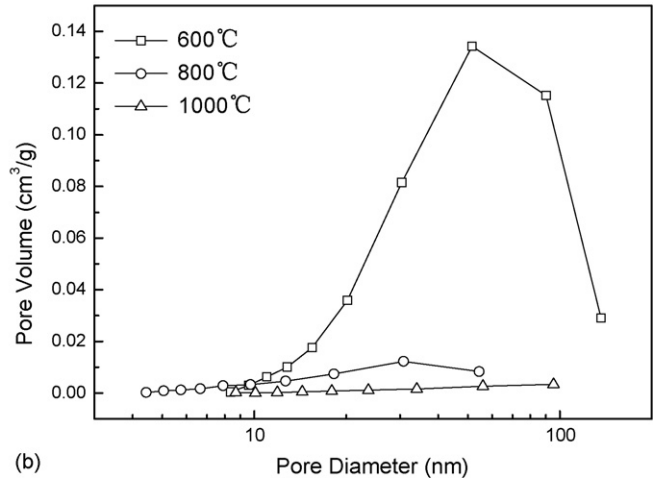


Fig. 5. (a) $N_2$ adsorption isotherms and (b) PSD (pore size distribution) plots of the fir-templated ZnO sample calcined at 600, 800, 1000 °C.

vaporize into as well as from the surface of the microparticle at the beginning of desorption. According to the analysis of FESEM and TEM results, the increased calcination temperature resulted in the increment of pore size. So the isotherms of 800 and 1000 °C samples change to type II without hysteresis loop which is the characteristic of nonporous or macroporous absorbents and unrestricted monolayer–multilayer absorption. Combining with the observation results of FESEM, the type II hysteresis loop is mainly attributed to the macroporous structures of flake ZnO.

Fig. 6 illustrates the cathodoluminescence (CL) spectra of the four fir-templated flake ZnO samples with calcination temperatures from 600 to 1200 °C. The typical two emission peaks of a narrow, weak UV near-band-emission and a broad, strong deep-level emission are observed in the CL spectra. The UV emission locates at about 390 nm, which is considered to be originated from the radiative recombination of free excitons.

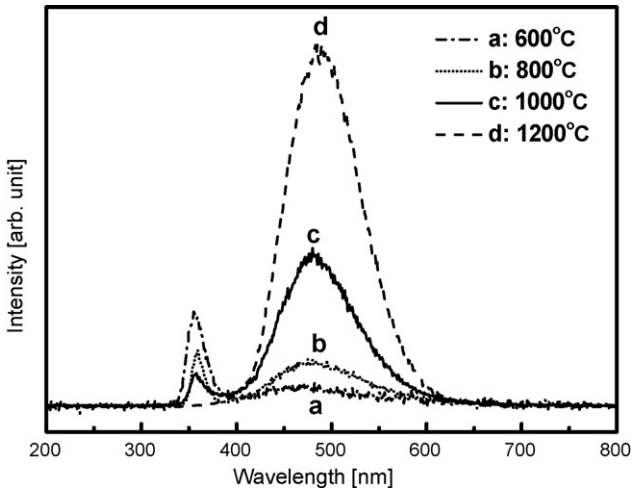


Fig. 6. Cathodoluminescence (CL) spectra of the fir-templated samples calcined at 600, 800, 1000 and 1200 °C separately.

The intensity of UV emission decreases with rising of calcination temperature and disappeared at 1200 °C finally, which can be attributed to the quantum confinement effect [22]. The particle size of ZnO increases from 20 to 50 nm to about several μm with the calcination temperature increasing from 600 to 1200 °C. As a result of particle size increasing, the energy band gap between ground state and the first excited state of the excitons was increased, which caused transition and recombination probability of excitons to be reduced, so that UV emission intensity was decreased.

The broad visible band here is a strong temperature-dependent emission. With rising temperature, the blue emission band became more intense and sharper and the peak position red-shifted slightly from about 475 to 490 nm. The shift towards higher energy with decreasing particle size is also caused by the quantum confinement effect because smaller particles lead to broader forbidden band for recombination. The mechanism behind visible luminescence has not been established, despite numerous studies which have considered intrinsic defects [23] (interstitial zinc ions or oxygen vacancies), zinc vacancies [24], and oxygen vacancies [25] to be the recombination centers. Oxygen vacancies are considered as the most likely candidates for the recombination centers in the blue emission of ZnO. The electron transition from shallow donors of oxygen vacancies to the valence band is the origin of this emission. When $Zn(NO_3)_2$ decomposed from 340 to 440 °C during calcination, ZnO was produced accompanied by plentiful oxygen vacancies which became dominant intrinsic defect of ZnO crystal. But high carrier concentration of n-type ZnO can cause luminescence quenching due to Auger effect. Heat treatment can reduce defects and oxygen vacancies and bring about better crystal, which can strengthen visible radiation based on the band edge transition. The radiation process is accompanied by non-radiative recombination and phonon emission, which affects the intensity of visible emission strongly. The defects are considered as the centers of nonradiative recombination. So the better crystal structure and fewer defects also can reduce the nonradiative recombination. As a result of two reasons, the intensity of blue emission becomes much higher with rising temperature.

## 4. Conclusions

Fir-templated ZnO products have been prepared successfully by a simple biotemplated process. Fir's tracheid and pit structures were inherited by ZnO samples. Through adjusting calcination temperature, the pores and ZnO grains have different morphologies and size in both bulk and flake ZnO samples. The pore sizes of fir-templated ZnO samples decrease from 20 μm in 600 °C calcined bulk sample to 10 μm in 1200 °C calcined bulk sample, and increase from 50 nm to several μm in flake samples at the same time. CL spectra indicate luminescence properties at both UV and blue bands. It is found that the UV emission can be attributed to the radiative recombination of free excitons, while blue emission depends on oxygen vacancies as the recombination centers. The increase of calcination temperature plays a key role for the luminescence property, causing the UV emission intensity to go down due to quantum confinement effect and the blue emission to go up due to fewer defects. We predict the wood anatomy also can affect the CL behavior of wood-templated ZnO, which is still in research.

## Acknowledgements

The authors wish to express their thanks to the financial support of National Natural Science Foundation of China (No. 50371055), Major Project on Basic research of Shanghai (No. 04DZ14002), Fok Ying Tung Education Fund (No. 94010), Program for New Century Excellent Talents in university(NCET-04-0387), Nano-research Program of Shanghai (No. 0452nm045) and National Basic Research Program of China (No. 2006CB601200).

## References

[1] R.K. Thareja, A. Mitra, Random laser action in ZnO, Appl. Phys. B 71 (2) (2000) 181–184.
[2] X.Q. Zhang, Z.K. Tang, M. Kawasaki, A. Ohtomo, H. Koinuma, Resonant exciton second-harmonic generation in self-assembled ZnO microcrystallite thin films, J. Phys.: Condens. Matter 15 (2003) 5191–5196.
[3] M. Lorenz, J. Lenzner, E.M. Kaidashev, H. Hochmuth, M. Grundmann, Cathodoluminescence of selected single ZnO nanowires on sapphire, Ann. Phys. (Leipzig) 13 (1–2) (2004) 39–42.
[4] Z.W. Pan, Z.R. Dai, Z.L. Wang, Nanobelts of semiconducting oxides, Science 291 (2001) 1947–1949.
[5] M.J. Zheng, L.D. Zhang, G.H. Li, W.Z. Shen, Fabrication and optical properties of large-scale uniform zinc oxide nanowire arrays by one-step electrochemical deposition technique, Chem. Phys. Lett. 363 (1/2) (2002) 123–128.
[6] H.J. Fan, W. Lee, R. Scholz, A. Dadgar, A. Krost, K. Nielsch, M. Zacharias, Arrays of vertically aligned and hexagonally arranged ZnO nanowires: a new template-directed approach, Nanotechnology 16 (2005) 913–917.
[7] B.P. Zhang, N.T. Binh, Y. Segawa, K. Wakatsuki, N. Usami, Optical properties of ZnO rods formed by metalorganic chemical vapor deposition, Appl. Phys. Lett. 83 (8) (2003) 1635–1637.
[8] S. Mann, Biomineralization and biomimetic materials chemistry, J. Mater. Chem. 5 (1995) 935–946.
[9] P. Greil, Biomorphous ceramics from lignocellulosics, J. Eur. Ceram. Soc. 21 (2) (2001) 105–118.
[10] L. Esposito, D. Sciti, A. Piancastelli, A. Bellosi, Microstructure and properties of porous beta-SiC templated from soft woods, J. Eur. Ceram. Soc. 24 (2) (2004) 533–540.
[11] J. Ding, B.H. Sun, T.X. Fan, D. Zhang, M. Kamada, H. Oqawa, Q.X. Guo, EXAFS study on dynamic structural property of porous morph-genetic SiC, Nucl. Instrum. Meth. Phys. Res. Sect. B 238 (2005) 138–140.
[12] P. Greil, T. Lifka, A. Kaindl, Biomorphic cellular silicon carbide ceramics from wood: I. Processing and microstructure, J. Eur. Ceram. Soc. 18 (1998) 1961–1973.
[13] H. Sieber, C. Hoffmann, A. Kaindl, P. Greil, Biomorphic cellular ceramics, Adv. Eng. Mater. 2 (3) (2000) 105–109.
[14] B.H. Sun, T.X. Fan, D. Zhang, T. Okabe, The synthesis and microstructure of morph-genetic TiC/C ceramics, Carbon 42 (1) (2004) 177–182.
[15] Z.T. Liu, T.X. Fan, W. Zhang, D. Zhang, The synthesis of hierarchical porous iron oxide with wood templates, Microporous Mesoporous Mater. 85 (2005) 85–88.
[16] Z.T. Liu, T.X. Fan, D. Zhang, Synthesis of biomorphous nickel oxide from a pinewood template and investigation on a hierarchical porous structure, J. Am. Ceram. Soc. 89 (2) (2005) 662–665.

[17] J. Cao, C.R. Rambo, H. Sieber, Manufacturing of microcellular, biomorphous oxide ceramics from native pine wood, Ceram. Int. 30 (2004) 1967–1970.
[18] T. Ota, M. Imaeda, H. Takase, M. Kobayashi, N. Kinoshita, T. Hirashita, H. Miyazaki, Y. Hikichi, Porous titania ceramic prepared by mimicking silicified wood, J. Am. Ceram. Soc. 83 (6) (2000) 1521–1523.
[19] C. Zollfrank, R. Kladny, H. Sieber, P. Greil, Biomorphous SiOC/C-ceramic composites from chemically modified wood templates, J. Eur. Ceram. Soc. 24 (2) (2004) 479–487.
[20] C. Zollfrank, H. Sieber, Microstructure and phase morphology of wood derived biomorphous SiSiC-ceramics, J. Eur. Ceram. Soc. 24 (2) (2004) 495–506.
[21] N.A. Seaton, Determination of the connectivity of porous solids from nitrogen sorption measurements, Chem. Eng. Sci. 46 (1991) 1895–1909.
[22] L. Brus, Electronic wave-functions in semiconductor clusters—experiment and theory, J. Phys. Chem. 90 (1986) 2555–2560.
[23] Y.G. Wang, S.P. Lau, X.H. Zhang, H.W. Lee, S.F. Yu, B.K. Tay, H.H. Hng, Evolution of visible luminescence in ZnO by thermal oxidation of zinc films, Chem. Phy. Lett. 375 (2003) 113–118.
[24] A.F. Kohan, G. Ceder, D. Morgan, C.G. Van de Walle, First-principles study of native point defects in ZnO, Phys. Rev. B 61 (22-1) (2000) 15019–15027.
[25] K. Vanheusden, W.L. Warren, C.H. Seager, D.R. Tallant, J.A. Voigt, B.E. Gnade, Mechanisms behind green photoluminescence in ZnO phosphor powders, J. Appl. Phys. 79 (1996) 7983–7990.